ICEMS2008

ICEMS 2008
The International Conference on Electrical Machines and Systems

International Conference on Electrical Machines and Systems

Oct.17-20, 2008, Shangri-La Hotel, Wuhan, China

Search

Author name ▾ | Suk-Hee Lee | SEARCH » | CLEAR CONDITIONS »

- Keynote Speech
- Designing, Manufacturing, Testing and Standards
- Field Analysis and Computation
- High Field Magnet and Applications
- Particle Accelerator and Related Techniques
- Renewable Energy Generation
- Small & Micro Machines, Servos and Actuators
- Transformers, Reactors and Apparatus
- Conventional Machines: IM, Sync. and DC Machines, etc
- Education for Electric Machinery
- Heating, Cooling, Viberation, Noise and EMC
- Insulating, Monitoring, Diagnosis and Maintenance
- Power Electronics, Electric Drives and Motion Control
- Special Machines: PM Machines, RM&SRM, LM, etc
- Theroy, Modeling and Simulation

Tao Sun, Soon-O Kwon, Suk-Hee Lee, Jung-Pyo Hong Top

Investigation and Comparison of Inductance Calculation Methods in Interior Permanent Magnet Synchronous Motors

Suk-Hee Lee, Geun-Ho Lee, Sung-Il Kim, Jung-Pyo Hong Top

A Novel Control Method for Reducing Torque Ripple in PMSM Applied for Electric Power Steering

A Novel Control Method for Reducing Torque Ripple in PMSM applied for Electric Power Steering

Suk-Hee Lee, Geun-Ho Lee, Sung-Il Kim, Jung-Pyo Hong, Senior Member, IEEE
School of Mechanical Engineering, Hanyang University, Seoul 133-791, Korea

***Abstract*-This paper proposes a novel control method that uses current harmonics to minimize torque ripple for Permanent magnet Synchronous Motor (PMSM) applied to Electric Power Steering (EPS) system. In the EPS system, PMSM is accompanied by magnetic saturation of iron core due to high power and limited space. Partial magnetic saturation in the stator teeth results in significant torque ripple. In order to reduce output torque ripple, current harmonics calculated. Presented method is verified by experiments.**

I. INTRODUCTION

EPS system is a kind of steering system which depends upon the torque provided directly by electromotor. Recently the EPS system has been widely used in automobile. It enables us to reduce manufacturing cost and to improve fuel efficiency as compared with the traditional hydraulic power steering system [1][2]. PMSM has many advantages such as high efficiency, high torque per rotor volume and wide speed range. These merits make it particularly suitable for automotive and other applications where space and energy savings is critical [3]. In the column typed EPS system, PMSM is directly assembled to the steering shaft by a reduction gear so the motor vibration and torque fluctuations are directly transferred through the steering wheel to the hands of the driver. Because a driver feels torque fluctuations, only 1~3% ripple of rated torque will be permitted. Recent research focused on the motor design and control which has low cogging torque and torque fluctuations. [4]-[6]. As it is, there are a lot of technical papers that have presented the motor design and control technique. However, unlike them, this paper shows the estimation method of compensation current for suppressing torque ripple caused by the magnetic saturation in the PMSM. Due to the spatial limitation in the EPS application, the magnetic saturation in the stator core is inevitable in high torque region. This paper analyzes torque ripple generated by the partial saturation in the motor fabricated for the EPS. Furthermore, d-, q-axis inductance is measured to prove the saturation with the use of Discrete Fourier Transform (DFT). The harmonic current distribution which must be added to q-axis current to minimize torque ripple is calculated through Finite Element Analysis (FEA), and the effective method in the PMSM driver is proposed in order to create the harmonic current. In the end, the results are verified by test.

II. ANALYSIS MODEL

Fig. 1 shows a surface typed PMSM for the column typed EPS system. And the rotor configuration skewed in order to reduce cogging torque. The specification of PMSM are listed in Table I, and cogging torque and Total Harmonic Distortion (THD) of back-EMF required in the motor is less than 0.02Nm and 0.7% respectively. Fig. 2 displays the torque waveforms when the PMSM is driven with constant q-axis current. To measure torque ripple accurately, the motor is driven at 10rpm, and input current is controlled with THD less than 0.5%. The 6 times torque ripple of electric frequency is increased as the magnetic torque is higher. Therefore, even if it has good characteristics in the low torque region, the torque ripple generated at the rated torque can't be neglected.

An inductance measurement method is presented in order to demonstrate the magnetic saturation effect of PMSM. The effect can be observed from the stator winding terminals as the change of inductance. The inductance depends on the input current and the rotor position. The measurement of inductance is accomplished by using DFT with high frequency current injection and discussed in the following.

The equivalent circuit for the vector control of PMSM is based on a synchronously rotating reference frame, and the mathematical model of equivalent circuit is given as follow:

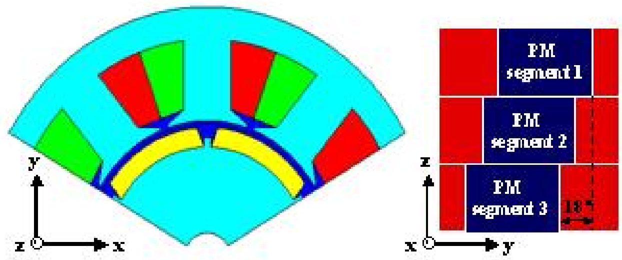

(a) 2D-FEM model (b) Permanent magnet shape

Fig. 1. 2D-FEM model and PM shape for the column typed EPS.

TABLE I
SPECIFICATION OF PMSM

Items	Value
TRV	80.1kNm/m^3
Br (@20~25 ℃)	1.35T
Number of poles and slots	6/9
Rated torque/ Rated current	4Nm/ 70A$_{rms}$
Base and Maximum speed	1000, 2000rpm

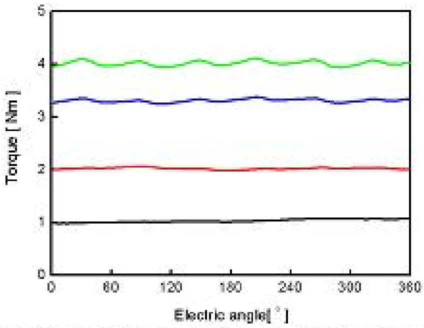

Fig. 2. Torque waveforms of PMSM measured at 10rpm.

$$\begin{bmatrix} v_d \\ v_q \end{bmatrix} = \begin{bmatrix} R_s + pL_d & -\omega_s L_q \\ \omega_s L_d & R_s + pL_q \end{bmatrix} \begin{bmatrix} i_d \\ i_q \end{bmatrix} + \begin{bmatrix} 0 \\ \omega_s \psi_a \end{bmatrix} \begin{bmatrix} i_d \\ i_q \end{bmatrix} \qquad (1)$$

where i_d, i_q: d, q components of armature current; v_d, v_q: d, q components of terminal voltage; ψ_a: $\sqrt{3/2}\ \psi_f$, ψ_f: maximum flux linkage of permanent magnet; R_s: armature winding resistance; L_d, L_q: inductance along d-, q-axis; $p = d/dt$.

The saturation phenomenon occurs in all three phases and can be transformed to the orthogonal d-q coordinates oriented toward a desired direction determined by the angle (θ). A high frequency alternating current is injected in the synchronously rotating frame, and the inductance is measured at each angle when PMSM is rotating. The d-axis behaves just as a resistance and inductance.

$$\frac{V_{dac}(\omega)}{I_{dac}(\omega)} = R + j\omega L_d \ , \ \omega L_d = imag\left\{\frac{V_{dac}(\omega)}{I_{dac}(\omega)}\right\} \qquad (2)$$

$$X(\omega_o) = \frac{1}{N}\sum_{n=0}^{N-1} x(nT_s)\cdot e^{-j\omega_o nT_s} = a_1 - jb_1 \qquad (3)$$

To measure the d-axis inductance at a given angle, the axis is excited with a periodic small signal having frequency ω_o and sampled N times per period. The value of commanded voltage and feedback current are measured at the excitation frequency of the small signal by using DFT. The inductance is calculated from the voltage and current coefficients after one or several periods of small signal excitation.

$$a_1 = \frac{1}{N}\sum_{n=0}^{N-1} x(nT_s)\cdot \cos\left(\omega_o nT_s\right) \qquad (4)$$

$$b_1 = \frac{1}{N}\sum_{n=0}^{N-1} x(nT_s)\cdot \sin\left(\omega_o nT_s\right) \qquad (5)$$

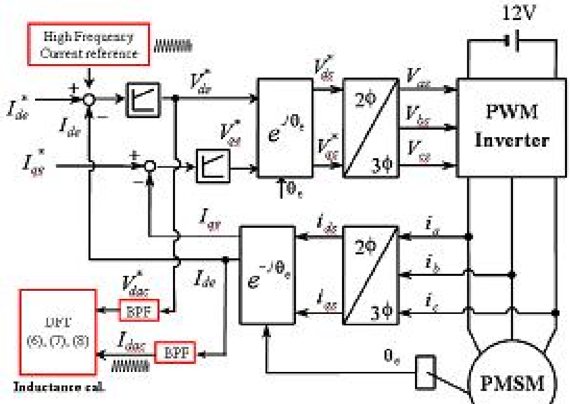

Fig. 3. Inductance measurement block diagram at vector control.

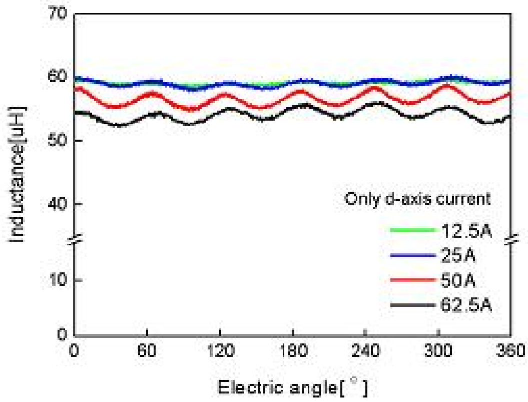

Fig. 4. D-axis inductance distribution according to electric angle.

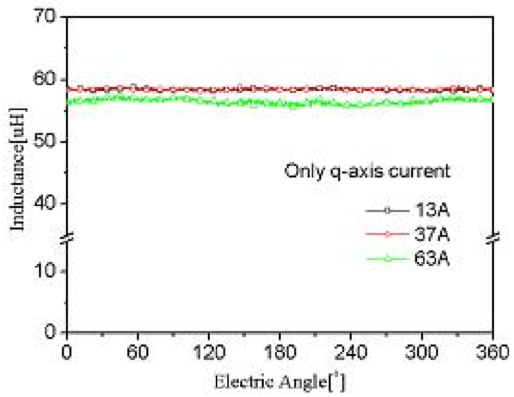

Fig. 5. Q-axis inductance distribution according to electric angle.

$$L_d = \frac{1}{\omega_o}\frac{a_{1Vd}\times b_{1Id} - a_{1Id}\times b_{1Vd}}{a_{1Id}^2 + b_{1Id}^2} \qquad (6)$$

where a_{1Id} and a_{1Vd} are the Fourier coefficient of current and voltage. Fig. 3 shows the block diagram of inductance measurement which has the high frequency current reference, BPF and DFT block in the vector controller.

The three percent of rated current with 500Hz are injected and I_{de} and V_{de} signals are filtered by BPF when the motor is running at low speed. D-, q-axis inductance is decreased according to

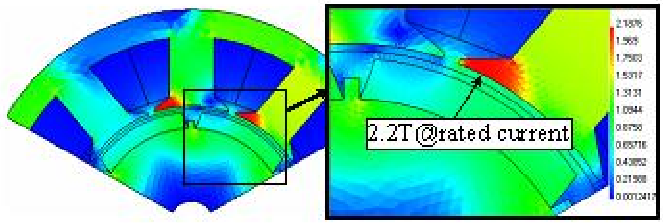

Fig. 6. Flux density distribution at 70A.

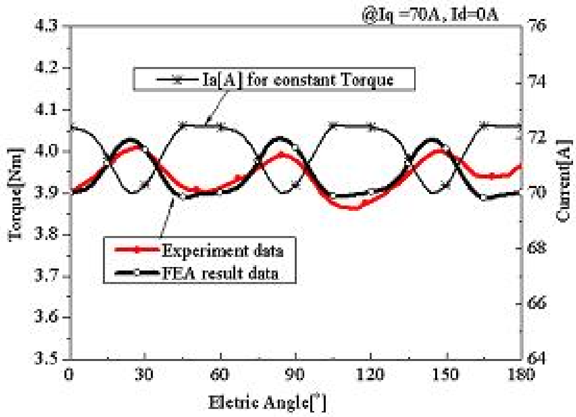

Fig. 7. Torque comparison of analysis and test result.

d-axis current increases, and it has 6 times fluctuation of electric frequency as shown in Fig. 4. We can find that the partial saturation of stator teeth makes 6 times torque ripple of electric frequency in the PMSM. Fig. 5 shows the q-axis inductance. Q-axis inductance has smaller variation compared with d-axis inductance.

III. Estimation Process of Compensation Current

In this paper, FEA is used in order to analyze the characteristics of PMSM and get the waveform of injection current to reduce torque pulsation. Nonlinear analysis considers the magnetic saturation of stator core. Fig. 6 shows the flux density distribution, and the maximum flux density of stator teeth indicates 2.2T at the rated current.

As shown in Fig. 7, the torque characteristics of PMSM are obtained by FEA, and the analysis result is compared to experimental result. The result at the rated current is similar to experimental result. In the test, the PMSM is rotated at low speed in order to drive the motor with a sinusoidal current. In this paper, the flow chart displayed in Fig. 8 is employed in order to obtain q-axis current distribution which minimizes torque ripple according to electric angle θ_e. FEA is iterated at the each rotor position with varying I_{qAC} to search the flat torque waveform.

$$i_q = i_{q0} + i_{qAC} \tag{7}$$

where i_{q0}: q component of armature current for the rated torque; i_{qAC}: compensation current added to i_{q0} in order to minimize torque ripple.

From this method, the compensation current which can minimize torque fluctuation is calculated according to current angle and expressed like Fig. 9. At the rated torque, 2.5A peak current is added to q-axis current.

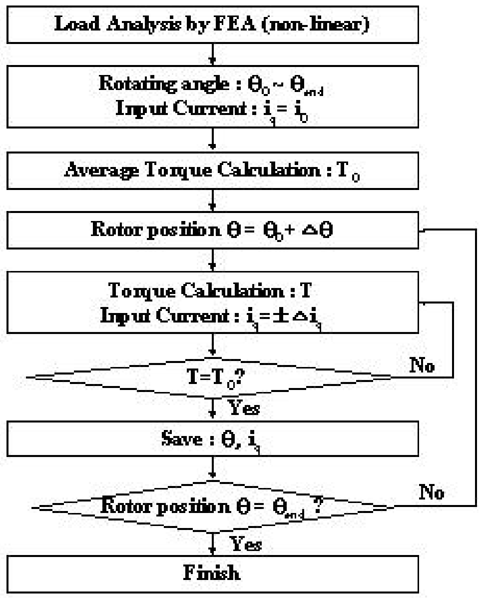

Fig. 8. Torque calculation procedure of the compensation current.

IV. FEA Analysis and Test Results

The compensation current according to a given torque is obtained like Fig. 10 while d-axis current is controlled to zero. As shown in Fig. 11, the harmonics of compensation current displayed in Fig. 11 consist of 6th, 12th, 18th, 24th and 30th harmonic component according to q-axis current. Therefore, if 18th, 24th and 30th harmonic component is neglected, the current can be simplified as the function of i_{q0}:

$$i_{qAC} = \sqrt{0.062 + 0.00028 i_{q0}^2} \cdot \cos(6\theta_e) + (0.071 + 0.0056 i_{q0}) \cdot \cos(12\theta_e) \tag{8}$$

Fig. 12 shows the effective real time compensation strategy to minimize torque ripple caused by magnetic saturation in the vector controller. From the test result, the 6 times torque harmonic of electric frequency is decreased to 30% as shown in Fig.13. By injecting the only 2% current of rated current, torque ripple caused by the partial saturation could be effectively suppressed.

V. Conclusion

This paper studies the torque ripple reduction method for the PMSM applied in EPS system. Due to the partial magnetic saturation in the stator teeth, the significant torque ripple may be generated in the PMSM. This magnetic saturation causes the inductance variation with different position, which can be obtained by measuring the real time inductance using the DFT. In this paper, the saturation effect was analyzed by a nonlinear analysis, and the simple compensation strategy to minimize the torque ripple at each electric angle was proposed. Finally, the validity of the analysis and compensation method was verified by test result of PMSM fabricated for the EPS, and with the method, the torque ripple caused by the magnetic saturation could be effectively reduced at the rated torque.

References

[1] Yoshifumi Morita, Kentaro Torii, Norio Tsuchida, Hiroyuki Ukai, Makoto Iwasaki, Nobuyuki Matsui, Jiro Hayashi, Noriyuki Ido and Hiroshi shikawa "Decoupling Control of Electric Power Steering System with Variable Gear Transmission System," *IEEE Industrial Electronics, IECON 2006 – 32nd Annual Conference on*, pp.5264-5269, November 2006.

[2] Xiong Jianqiao, Tang Xiaoqi, and Chen Jihong, "A Kind of Embedded Electric Power Steering System Based on DSP LF2407," *Mechatronic and Embedded Systems and Applications, Proceedings of the 2nd IEEE/ASME International Conference on*, pp.1-5, August 2006.

[3] Y.Shimizu, T.Kawai, " Development of Electric Power Steering", SAE Transactions, No, 1991-0014,1991

[4] M. S. Islam, S. Mir, T. Sebastian, and S. underwood, "Design considerations of sinusoidally excited permanent-magnet machaines for low-torque-ripple applications," *IEEE Trans. Ind. Applicat.*, vol. 41, no. 4, pp. 955-962, July 2005.

[5] P. Mattavelli, L. Tubiana, and M. Zigliotto, "Torque-ripple reduction in PM synchronous motor drives using repetitive current control," *IEEE Trans. Poewer Electron.*, vol. 20, no. 6, pp. 1423-1431, Nov. 2005.

[6] G. H. Lee, S. I. Kim, J. P. Hong, and J. H. Bhan, "Torque ripple reduction of interior permanent magnet synchronous motor using harmonic injected current," *IEEE Trans. Magn.*, to be published.

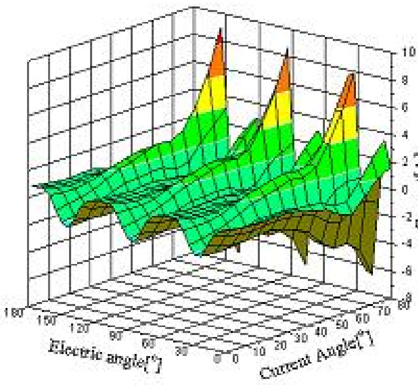

Fig. 9. Compensation current distribution according to current angle.

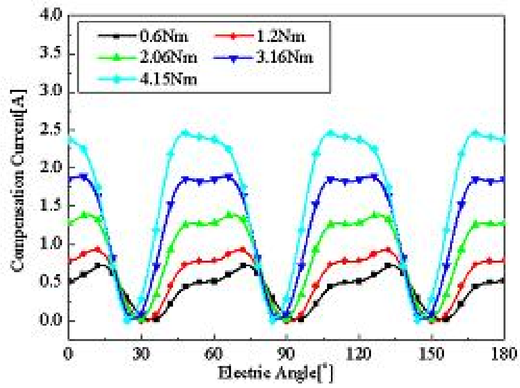

Fig. 10. Compensation current distribution according to a given torque.

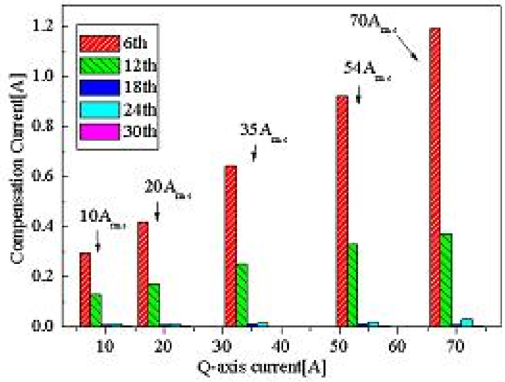

Fig. 11. Harmonic components of compensation current.

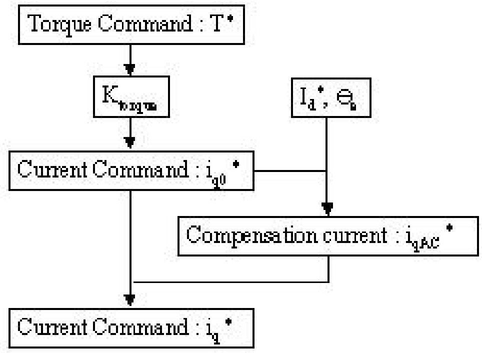

Fig. 12. Compensation strategy in the vector controller.

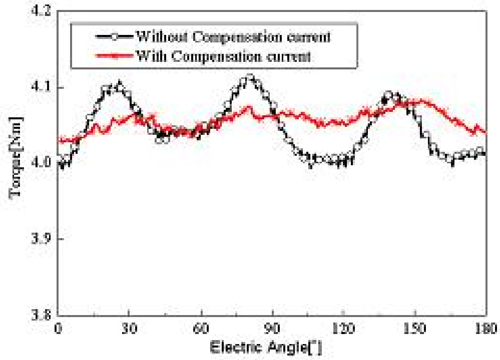

Fig. 13. Torque waveform at 70A.